

Hole Dynamics in Two-Dimensional Antiferromagnetic Mott Insulators

F.F. Assaad¹ and M. Imada²

¹ Institut für Theoretische Physik III,

Universität Stuttgart, Pfaffenwaldring 57, D-70550 Stuttgart, Germany.

² Institute for Solid State Physics, University of Tokyo,

7-22-1 Roppongi, Minato-ku, Tokyo 106, Japan.

The dispersion relation of a doped hole in the half-filled 2D Hubbard model is shown to follow a $|\vec{k}|^4$ law around the $(0, \pm\pi)$ and $(\pm\pi, 0)$ points in the Brillouin zone. Upon addition of pair-hopping processes this dispersion relation is unstable towards a $|\vec{k}|^2$ law. The above follows from $T = 0$ Quantum Monte calculations of the single particle spectral function $A(\vec{k}, \omega)$ on 16×16 lattices. We discuss finite dopings and argue that the added term restores coherence to charge dynamics and drives the system towards a $d_{x^2-y^2}$ superconductor.

PACS numbers: 71.27.+a, 71.30.+h, 71.10.+x

The excitation spectrum of a band insulator is gapped in both the spin and charge degrees of freedom. In this case the single particle Green function will essentially take a free particle form since there are no low lying excitations on which the added particle can scatter. The Mott insulator with long-range antiferromagnetic order has a charge gap but no spin gap. This leads to non-trivial hole dynamics which will depend on the dynamical spin susceptibility as well as on the coupling between spin and charge degrees of freedom. Hole dynamics in magnetic insulators have been addressed in the pioneering work of Brinkman and Rice [1]. Progress in photoemission spectroscopy has provided us with an experimental realization of this problem [2]. In this Letter, we show numerically that hole dynamics in a two-dimensional Mott insulator with long-range magnetic order may behave in radically different ways. The dispersion relation of a hole doped into the half-filled Hubbard model is very flat around the $(0, \pm\pi)$ and $(\pm\pi, 0)$ points in the Brillouin zone. We will give numerical evidence that it follows a $|\vec{k}|^4$ law. We argue that this flatness and resultant singular momentum dependence of charge excitations provides us with a microscopic basis for understanding incoherent charge dynamics and unusual character of the metal-insulator transition. Upon addition of a term with matrix element W which describes pair-hopping processes, this flat dispersion relation is unstable towards a $|\vec{k}|^2$ law. Although the added term for *small* values of W does not alter the insulating state itself it restores coherence to charge dynamics in the vicinity of the Mott transition.

The model we consider reads:

$$H_{tUW} = -\frac{t}{2} \sum_{\vec{i}} K_{\vec{i}} + U \sum_{\vec{i}} \tilde{n}_{\vec{i},\uparrow} \tilde{n}_{\vec{i},\downarrow} - W \sum_{\vec{i}} K_{\vec{i}}^2 \quad (1)$$

where

$$K_{\vec{i}} = \sum_{\sigma, \vec{\delta}} \left(c_{\vec{i},\sigma}^\dagger c_{\vec{i}+\vec{\delta},\sigma} + c_{\vec{i}+\vec{\delta},\sigma}^\dagger c_{\vec{i},\sigma} \right). \quad (2)$$

Here $\vec{\delta} = \pm\vec{a}_x, \pm\vec{a}_y$, $c_{\vec{i},\sigma}^\dagger$ creates an electron with z -

component of spin σ on lattice site \vec{i} and $\tilde{n}_{\vec{i},\sigma} = c_{\vec{i},\sigma}^\dagger c_{\vec{i},\sigma} - 1/2$. We consider a square lattice of linear size L and impose periodic boundary conditions in both lattice directions. The t - U - W model has been introduced and studied in Ref. [3–6]. The results show that at half-filling and finite values of U/t , W triggers a quantum transition between the Mott insulator and a $d_{x^2-y^2}$ superconductor.

To understand the influence of the W -term on hole dynamics it is convenient to consider the strong coupling limit where double occupancy is prohibited. In this limit, the W -term describes pair-hopping processes in the spin singlet, $-W \sum_{i,\vec{\delta},\vec{\delta}'} \left(T_{i,\vec{\delta}}^\dagger \Delta_{i,\vec{\delta}'} + \Delta_{i,\vec{\delta}} \Delta_{i,\vec{\delta}'}^\dagger \right)$ and spin triplet $W \sum_{i,\vec{\delta},\vec{\delta}',m} \left(T_{i,\vec{\delta},m}^\dagger T_{i,\vec{\delta}',m} + T_{i,\vec{\delta},m} T_{i,\vec{\delta}',m}^\dagger \right)$ channels. Here, $\Delta_{i,\vec{\delta}}^\dagger = \left(c_{i,\uparrow}^\dagger c_{i+\vec{\delta},\downarrow}^\dagger - c_{i+\vec{\delta},\downarrow}^\dagger c_{i,\uparrow}^\dagger \right) / \sqrt{2}$ and $T_{i,\vec{\delta},m}^\dagger$ creates a spin triplet on the bond \vec{i} , $\vec{i} + \vec{\delta}$ with z -component of spin m . In the strong coupling limit, the states $T_{i,\vec{\delta},m}^\dagger$ and $\Delta_{i,\vec{\delta}}^\dagger$ form a complete basis for a pair of electrons on the bond \vec{i} , $\vec{i} + \vec{\delta}$. Thus, any spin configuration surrounding a hole may be written as a superposition of triplets and singlets on a set of bonds covering the lattice. One may now see how hole dynamics are effected by the W -term: the motion of a pair of electrons is nothing but the hopping of a hole within the same sublattice accompanied by a local rearrangement of spins. Due to zero point quantum fluctuations of the spin background, the resultant state is not orthogonal to the ground state. Since the state in which the hole is doped has antiferromagnetic order, we expect the *singlet* pair-hopping processes to dominate the low-energy physics. Those processes are similar to the three site term obtained in a strong coupling expansion of the Hubbard model [7]. The influence of those terms on hole dynamics has been addressed in Ref. [8].

At half-band filling auxiliary field quantum Monte Carlo (QMC) simulations provide an efficient tool for the study of the above model. Partly due to the presence of particle-hole symmetry, the infamous sign prob-

lem is avoidable. Our $T = 0$ data are produced with the projector QMC (PQMC) algorithm [9,10] supplemented with a numerically stable method to compute imaginary time displaced correlation functions [11]. The imaginary time data is analytically continued to the real axis with the Maximum-Entropy method [12,13]. We have used a flat default model and taken into account correlations in imaginary time data with the use of the covariance matrix.

We start by considering the half-filled Hubbard model at $U/t = 4$ and $T = 0$. For this parameter set and after extrapolation to the thermodynamic limit numerical simulations lead to the conclusion that the ground state is an insulator with single particle gap $\Delta_{qp} = 0.67 \pm 0.015$ [14] and long-range antiferromagnetic order: $m \equiv \lim_{L \rightarrow \infty} \sqrt{3 \langle m_z((L/2, L/2)) m_z(\vec{0}) \rangle} = 0.39(5)$ [15,16]. Here, $m_z(\vec{i}) = \tilde{n}_{\vec{i},\uparrow} - \tilde{n}_{\vec{i},\downarrow}$. Fig. 1 plots $A(\vec{k}, \omega) \equiv \text{Im}G(\vec{k}, \omega)$, where $G(\vec{k}, \omega)$ corresponds to the single-particle Green function. Due to particle-hole symmetry, $A(\vec{k}, \omega) \equiv A(\vec{k} + \vec{Q}, -\omega)$ with $\vec{Q} = (\pi, \pi)$ in units of the lattice constant. The sum rule: $\int_{-\infty}^0 A(\vec{k}, \omega) d\omega = \pi \sum_{\sigma} \langle c_{\vec{k},\sigma}^{\dagger} c_{\vec{k},\sigma} \rangle$ is satisfied. We are primarily interested in the single-hole dispersion relation $E(\vec{k})$ as defined by the peak position in $A(\vec{k}, \omega)$. Around the $(0, \pi)$ and three equivalent points in the Brillouin zone, $E(\vec{k})$ shows a very flat structure. Along the $(0, 0)$ to $(0, \pi)$ direction $E(\vec{k})$ is compatible with a $|\vec{k}|^4$ law over an acceptable range (see Fig. 3). The same conclusion is reached when considering the (π, π) to $(0, \pi)$ direction. Such a flat dispersion relation has been observed numerically in t - J model calculations [17]. The overall flatness appears consistently with the flat dispersion observed in underdoped cuprates [2,18,19]. The following points are of interest. i) The energy difference $\Delta E = E(\vec{k} = (\pi/2, \pi/2)) - E(\vec{k} = (0, \pi))$ is not unambiguously distinguishable from zero within our resolution. $\Delta E = 0.045t, 0.06t$ and $0.015t$ for the $L = 8, 12$ and $L = 16$ lattices respectively. The uncertainty of our data, is in the same ballpark as the above quoted values. We note that the flatness of the dispersion relation around the $(0, \pi)$ point should lead to a broader lineshape at $(0, \pi)$ than at $(\pi/2, \pi/2)$ [20] thus leading to some ambiguity in the definition of $E(\vec{k})$. In fact, defining $E(\vec{k})$ as the leading edge rather than the peak position yields a negative value for ΔE for the $L = 16$ lattice. Lineshapes are notoriously hard to compute with the Maximum-Entropy method and further large scale calculations are required to confirm this point. ii) A shadow-band due to the presence of long-range magnetic order is seen along the $(\pi/2, \pi/2)$ to (π, π) to $(\pi, 0)$ direction. Around the $(0, 0)$ point a two *peak* feature is seen in the data. A similar feature at larger couplings is seen in Ref. [21].

We now set $W/t = 0.15$ and keep the other parame-

ters constant, $U/t = 4, T = 0, \langle n \rangle = 1$. At this point in parameter space, the ground state remains a Mott insulator with $m = 0.24(1)$ and $\Delta_{qp} = 0.54(6)$ [5]. Fig. 2 plots $A(\vec{k}, \omega)$ again on a $L = 16$ lattice. The following points are of importance. i) Upon inspection one notices that the bandwidth is substantially enhanced by the inclusion of the W -term. This high energy phenomena may be captured at a mean-field level by the Ansatz: $\langle n_{\vec{i},\uparrow} \rangle + \langle n_{\vec{i},\downarrow} \rangle = 1, \langle n_{\vec{i},\uparrow} \rangle - \langle n_{\vec{i},\downarrow} \rangle = (-m_{HF})^{i_x + i_y}$ and $\langle K_{\vec{i}} \rangle = K$. Self-consistency yields the single particle gap $\Delta_{HF} \equiv Um_{HF}/2 = 0.43t$ and a band ranging from $-11.9t$ to $11.9t$. The bandwidth agrees well with the Monte-Carlo data. This approximation *underestimates* the single particle gap thus showing that it does not capture the low-energy physics contained in the W -term. ii) Around the $(0, \pi)$ point, $E(\vec{k})$ is not as flat as for the Hubbard model. As shown in Fig. 3, the data is compatible with a quadratic fit. To be more precise, as W/t is enhanced the domain in \vec{k} -space around the $(0, \pm\pi), (\pm\pi, 0)$ points which is compatible with a $|\vec{k}|^4$ fit is suppressed. iii) As in Fig 1 the shadow-band feature is present. iv) The energy difference in the dispersion relation between the $(\pi/2, \pi/2)$ and $(0, \pi)$ points is not distinguishable from zero. [22]

Next we study finite dopings. Here, we are confronted to a sign problem so that the CPU time required to achieve a given precision scales exponentially with inverse temperature (β) and lattice size. The presented data is produced with the finite temperature QMC method [23,16]. We first consider the vertex contribution to pairing correlations in the d -wave and extended s -wave channels. This quantity is defined by:

$$P_{d,s}^v(\vec{r}) = \langle \Delta_{d,s}^{\dagger}(\vec{r}) \Delta_{d,s}(\vec{0}) \rangle - \sum_{\sigma, \vec{\delta}, \vec{\delta}'} f_{d,s}(\vec{\delta}) f_{d,s}(\vec{\delta}') \quad (3)$$

$$\left(\langle c_{\vec{r},\sigma}^{\dagger} c_{\vec{\delta}',\sigma} \rangle \langle c_{\vec{r}+\vec{\delta},-\sigma}^{\dagger} c_{\vec{0},-\sigma} \rangle + \langle c_{\vec{r},\sigma}^{\dagger} c_{\vec{0},\sigma} \rangle \langle c_{\vec{r}+\vec{\delta},-\sigma}^{\dagger} c_{\vec{\delta}',-\sigma} \rangle \right)$$

where $\Delta_{d,s}^{\dagger}(\vec{r}) = \sum_{\sigma, \vec{\delta}} f_{d,s}(\vec{\delta}) \sigma c_{\vec{r},\sigma}^{\dagger} c_{\vec{r}+\vec{\delta},-\sigma}^{\dagger}$, $f_s(\vec{\delta}) = 1$ and $f_d(\vec{\delta}) = 1(-1)$ for $\vec{\delta} = \pm \vec{a}_x$ ($\pm \vec{a}_y$). Per definition, in the absence of interaction $P_{d,s}^v$ vanishes (i.e. in the above mentioned mean field approximation which takes into account band width effects, $P_{d,s}^v$ vanishes.) Due to the strong variation of $P_{d,s}^v(\vec{0})$ [24] as a function of doping, we consider the quantity: $\tilde{P}_{d,s}^v(\vec{r}) = P_{d,s}^v(\vec{r})/P_{d,s}^v(\vec{0})$ which measures the *decay* rate. This quantity is plotted versus doping in Fig. 4. At the largest distance on our 8×8 lattice, the W -term substantially enhances the d -wave signal. We note that the same conclusion is reached when considering $P_{d,s} = \langle \Delta_{d,s}^{\dagger}(\vec{r}) \Delta_{d,s}(\vec{0}) \rangle$.

The uniform spin susceptibility is plotted versus temperature in Fig. 5(a) at $\langle n \rangle = 0.78, U/t = 4$, for various values of W/t . Starting from the noninteracting case ($U=W=0$) and turning on the Coulomb repulsion to $U/t = 4$ enhances the spin susceptibility. At *high* tem-

peratures, this enhancement may be understood within the random phase approximation. As W/t grows, there is a suppression of the spin susceptibility. There are two effects which cause this suppression. i) The enhancement of the bandwidth as a function of W/t . ii) The growth of d -wave pair correlations. Disentangling the contribution of those two effects at different energy scales is non-trivial. The spin structure factor $S(\vec{q}) \equiv \langle m_z(\vec{q})m_z(-\vec{q}) \rangle$ is plotted in Fig. 5 (b). The reduction of $S(\vec{q})$ at $\vec{q} = 0$ as W/t is enhanced may be traced back to our discussion of the spin susceptibility since the latter quantity is given by $\beta S(\vec{q} = 0)$. In the vicinity of $\vec{q} = (\pi, \pi)$, $S(\vec{q})$ shows a somewhat sharper feature at $W/t = 0.15$ than at $W/t = 0$, thus showing that the magnetic length scale is *enhanced* by the W -term.

In summary, we considered the t - U - W model at $U/t = 4$ and for two different choices of W : $W/t = 0$, $W/t = 0.15$. In both cases, the ground state at half-filling is a Mott insulator with long-range antiferromagnetic order. However, the nature of hole dynamics in this antiferromagnetic background is strongly dependent on the choice of W/t . In the case of the Hubbard model we concluded that the hole dispersion relation is consistent with a $|\vec{k}|^4$ law around the $(0, \pm\pi)$ and $(\pm\pi, 0)$ points in the Brillouin zone. This flat dispersion relation is compatible with the picture of incoherent charge dynamics and introduces a singular momentum dependence in the electron self-energy. Recently, the authors of Ref. [25,26] have computed the Drude weight on t - J clusters and found results consistent $D \sim \delta^2$. The sum rule for the optical conductivity is proportional to the doping δ in the case of the t - J model. Thus, close to the metal insulator transition, only a vanishingly small portion of the weight in the optical conductivity will be contained in the coherent Drude response. Introducing the W -term alters this situation. On one hand we have shown here that the dispersion relation around the $(0, \pm\pi)$ and $(\pm\pi, 0)$ points follow a $|\vec{k}|^2$ law. On the other hand, the Drude weight satisfies $D \sim \delta$ for the t - J - W model [25,26]. Thus, the W -term restores coherence to charge dynamics in the vicinity of metal-insulator transition. However, the short-range antiferromagnetic spin correlations at finite doping remain robust upon switching on W . In the doped phase, d -wave pairing correlations functions are substantially enhanced by the inclusion of W thus lending support to the occurrence of a superconducting state. In terms of quantum phase transitions the inclusion of the W -term alters the dynamical exponent from $z = 4$ to $z = 2$ [27,5,25,26]. More generally, the W -term exploits one of the many potential instabilities of the incoherent metallic state realized in the Hubbard model in the vicinity of the metal-insulator transition. As a more realistic model for high- T_c cuprates, smaller values of W are to be considered so as to study the interplay between the pairing energy scale and the larger energy scale associated with the flat

bands.

The numerical simulations were performed at the Supercomputer Center of the Institute for Solid State Physics, University of Tokyo, the HLRS-Stuttgart and HLRZ-Jülich. We thank M. Brunner, A. Muramatsu, H. Tsunetsugu and M. Zacher for conversations.

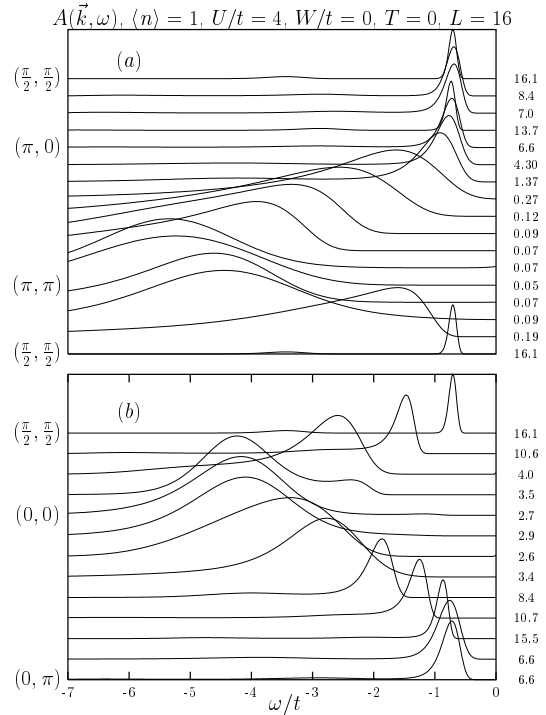


FIG. 1. $A(\vec{k}, \omega)$ at $T = 0$ for the half-filled Hubbard model at $U/t = 4$ on a 16×16 lattice. The considered path in the Brillouin zone is listed on the left hand side of the figure. We have normalized the raw data by the factor listed on the right hand side of the figure. This normalization sets the peak value of $A(\vec{k}, \omega)$ to unity for all considered \vec{k} vectors.

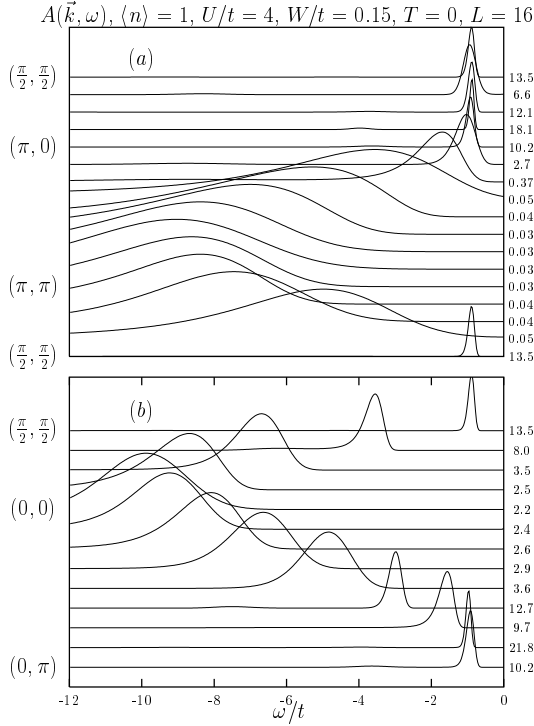


FIG. 2. Same as Fig. 1 but for $W/t = 0.15$.

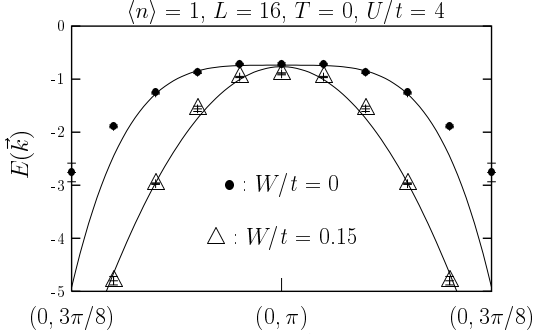


FIG. 3. Dispersion relation, $E(\vec{k})$, as defined by the peak position in $A(\vec{k}, \omega)$. The solid lines correspond to a least square fit to the form $a + b(\pi - k_y)^2$ ($a + b(\pi - k_y)^4$) for $W/t = 0$ ($W/t = 0.15$). For the fit we consider the k_y range $[5\pi/8, \pi]$ for both choices of W/t .

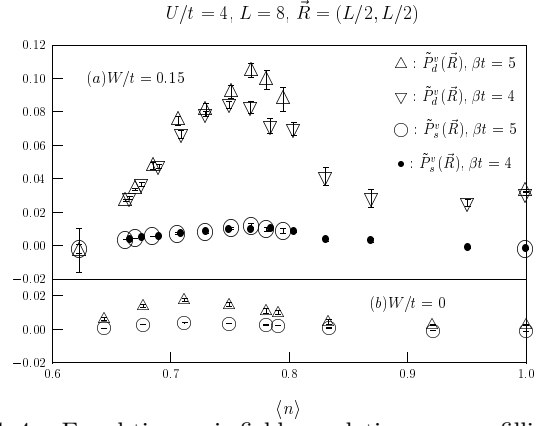


FIG. 4. Equal-time pair field correlations versus filling in the d -wave and extended s -wave channels. $\tilde{P}_{d,s}^v(\vec{R}) \equiv P_{d,s}^v(\vec{R})/P_{d,s}^v(\vec{0})$. The same scale is used for both (a) $W/t = 0.15$ and (b) $W/t = 0$.

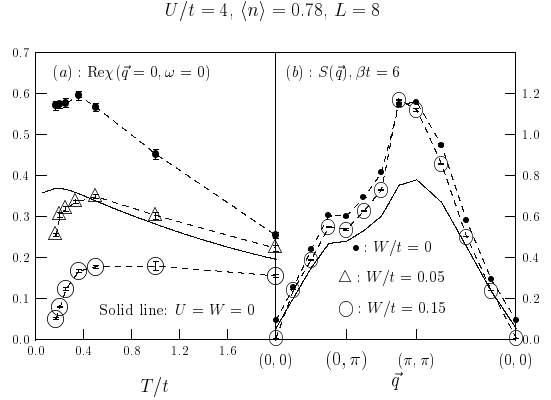


FIG. 5. (a) Spin susceptibility versus temperature for various values of W/t and $\langle n \rangle = 0.78$. (b) Spin structure factor at $\beta t = 6$, $\langle n \rangle = 0.78$ for the Hubbard and t - U - W models. In both (a) and (b) the solid line corresponds to the non-interacting ($U = W = 0$) case.

[1] W. F. Brinkman and T. M. Rice, Phys. Rev. B. **2**, 1324 (1970).
[2] B. O. Wells *et al.*, Phys. Rev. Lett. **74**, 964 (1995).
[3] F. F. Assaad, M. Imada, and D. J. Scalapino, Phys. Rev. Lett **77**, 4592 (1996).
[4] F. F. Assaad, M. Imada, and D. J. Scalapino, Phys. Rev. B **56**, 15001 (1997).
[5] F. F. Assaad and M. Imada, Phys. Rev. B **58**, 1845 (1998).
[6] F. F. Assaad, cond-mat/9806306 .
[7] J. E. Hirsch, Phys. Rev. Lett. **54**, 1317 (1985).
[8] K. J. von Szczepanski, P. Horsch, W. Stephan, and M. Ziegler, Phys. Rev. B. **41**, 2017 (1990).
[9] G. Sugiyama and S. Koonin, Anals of Phys. **168**, 1

- (1986).
- [10] S. Sorella, S. Baroni, R. Car, and M. Parrinello, Europhys. Lett. **8**, 663 (1989).
 - [11] F. F. Assaad and M. Imada, J. Phys. Soc. Jpn. **65**, 189 (1996).
 - [12] W. von der Linden, Applied Physics A **60**, 155 (1995).
 - [13] M. Jarrell and J. Gubernatis, Physics Reports **269**, 133 (1996).
 - [14] F. F. Assaad and M. Imada, Phys. Rev. Lett **76**, 3176 (1996).
 - [15] J. E. Hirsch and S. Tang, Phys. Rev. Lett. **62**, 591 (1989).
 - [16] S. White *et al.*, Phys. Rev. B **40**, 506 (1989).
 - [17] E. Dagotto, A. Nazarenko, and M. Boninsegni, Phys. Rev. Lett. **73**, 728 (1994).
 - [18] K. Gofron *et al.*, Phys. Rev. Lett. **73**, 3302 (1994).
 - [19] Z. X. Shen and D. S. Dessau, Phys. Rep. **253**, 1 (1995).
 - [20] Z. X. Shen and J. R. Schrieffer, Phys. Rev. Lett. **78**, 1771 (1997).
 - [21] R. Preuss, W. Hanke, and W. von der Linden, Phys. Rev. Lett. **75**, 1344 (1995).
 - [22] Thus, both considered models do not seem capable of reproducing the experimentally observed energy difference of $\sim 0.3eV$ for $Sr_2CuO_2Cl_2$ and $\sim 0.1eV$ for $La_{1.97}Sr_{0.03}CuO_4$ (A. Ino *et al.* private communication) between the $(0, \pi)$ and $(\pi/2, \pi/2)$ points in the Brillouin zone [2]. A theoretical explanation of this effect has been proposed by [28].
 - [23] J. E. Hirsch, Phys. Rev. B **31**, 4403 (1985).
 - [24] For the parameter set $\beta t = 5$, $W/t = 0.15$ and $U/t = 4$, $P_v^d(\vec{0}) \sim 1.00$ and $P_v^s(\vec{0}) \sim 1.04$ at $\langle n \rangle = 1$ whereas $P_v^d(\vec{0}) \sim 0.06$ and $P_v^s(\vec{0}) \sim 0.24$ at $\langle n \rangle \sim 0.62$. That the s -wave correlation dominates the short range has been discussed in Ref. [6].
 - [25] H. Tsunetsugu and M. Imada, J. Phys. Soc. Jpn. **67**, 1864 (1998).
 - [26] M. Imada, F. F. Assaad, H. Tsunetsugu, and Y. Motome, cond-mat/9808044 .
 - [27] M. Imada, A. Fujimori, and Y. Tokura, Rev. Mod. Phys. **70**, 1039 (1998).
 - [28] R. Eder, Y. Ohta, and G. A. Sawatzky, Phys. Rev. B. **55**, 3414 (1997).